Check for updates

Received: 13 April 2023 | Accepted: 22 May 2023

DOI: 10.1111/gcb.16811

Global Change Biology WILEY

RESEARCH ARTICLE

Long-term elevated precipitation induces grassland soil carbon loss via microbe-plant–soil interplay

Mengmeng Wang[1,2] | Xin Sun[2,3,4,5] | Baichuan Cao[1] | Nona R. Chiariello[6] | Kathryn M. Docherty[7] | Christopher B. Field[8] | Qun Gao[2] | Jessica L. M. Gutknecht[9] | Xue Guo[2,10] | Genhe He[11] | Bruce A. Hungate[12] | Jiesi Lei[2] | Audrey Niboyet[13,14] | Xavier Le Roux[15] | Zhou Shi[10] | Wensheng Shu[1] | Mengting Yuan[10] | Jizhong Zhou[10,16,17,18] | Yunfeng Yang[2]

[1]Institute of Ecological Science and Guangdong Provincial Key Laboratory of Biotechnology for Plant Development, School of Life Sciences, South China Normal University, Guangzhou, China

[2]State Key Joint Laboratory of Environment Simulation and Pollution Control, School of Environment, Tsinghua University, Beijing, China

[3]Department of Ecology and Evolutionary Biology, Yale University, New Haven, Connecticut, USA

[4]Yale Institute for Biospheric Studies, Yale University, New Haven, Connecticut, USA

[5]Department of Global Ecology, Carnegie Institution for Science, Stanford, California, USA

[6]Jasper Ridge Biological Preserve, Stanford University, Stanford, California, USA

[7]Department of Biological Sciences, Western Michigan University, Kalamazoo, Michigan, USA

[8]Stanford Woods Institute for the Environment, Stanford University, Stanford, California, USA

[9]Department of Soil, Water, and Climate, University of Minnesota, Saint Paul, Minnesota, USA

[10]Institute for Environmental Genomics, Department of Microbiology and Plant Biology, University of Oklahoma, Norman, Oklahoma, USA

[11]School of Life Sciences, Key Laboratory of Agricultural Environmental Pollution Prevention and Control in Red Soil Hilly Region of Jiangxi Province, Jinggangshan University, Ji'an, China

[12]Center for Ecosystem Science and Society, Department of Biological Sciences, Northern Arizona University, Flagstaff, Arizona, USA

[13]Institut d'Ecologie et des Sciences de l'Environnement de Paris, CNRS, INRAE, IRD, Sorbonne Université, Université Paris Cité, UPEC, Paris, France

[14]AgroParisTech, Palaiseau, France

[15]Laboratoire d'Ecologie Microbienne, INRAE, CNRS, VetAgroSup, UMR INRAE 1418, UMR CNRS, Université Lyon 1, Université de Lyon, Villeurbanne, France

[16]Earth and Environmental Sciences Division, Lawrence Berkeley National Laboratory, Berkeley, California, USA

[17]School of Civil Engineering and Environmental Sciences, University of Oklahoma, Norman, Oklahoma, USA

[18]School of Computer Science, University of Oklahoma, Norman, Oklahoma, USA

Correspondence
Jizhong Zhou, Institute for Environmental Genomics, Department of Microbiology and Plant Biology, University of Oklahoma, Norman, OK 73019, USA.
Email: jzhou@ou.edu

Yunfeng Yang, State Key Joint Laboratory of Environment Simulation and Pollution Control, School of Environment, Tsinghua University, Beijing 100084, China.
Email: yangyf@tsinghua.edu.cn

Funding information
G. Evelyn Hutchinson postdoctoral fellowship from Yale Institute for

Abstract

Global climate models predict that the frequency and intensity of precipitation events will increase in many regions across the world. However, the biosphere-climate feedback to elevated precipitation (eP) remains elusive. Here, we report a study on one of the longest field experiments assessing the effects of eP, alone or in combination with other climate change drivers such as elevated CO_2 (eCO_2), warming and nitrogen deposition. Soil total carbon (C) decreased after a decade of eP treatment, while plant root production decreased after 2 years. To explain this asynchrony, we found that the relative abundances of fungal genes associated with chitin and protein degradation

Mengmeng Wang and Xin Sun contributed equally.

 © 2023 John Wiley & Sons Ltd.

Biospheric Studies at Yale University; The Simons Foundation postdoctoral fellowship in Marine Microbial Ecology; Guangdong Basis and Applied Basic Research Foundation grant, Grant/Award Number: 2019A1515110345 and 2021A1515011497; Key Technology R&D Program of Jiangxi Province, Grant/Award Number: 20223BBG74S02; National Natural Science Foundation of China, Grant/Award Number: 41825016, 41877048 and 42007297; Office of Science and Office of Biological and Environmental Research (DOE-BER) of the U.S. Department of Energy Genomic Science Program, Grant/Award Number: DE-SC0004601 and DE-SC0010715; Office of the Vice President for Research at the University of Oklahoma; Science & Technology Fundamental Resources Investigation Program, Grant/Award Number: 2019FY100700; The French CNRS/INSU-EC2CO Program (project INTERACT); The French Institute of Agriculture, Food and Environment Research (INRAE, ECODIV Department); The Morgan Family Foundation; The Packard Foundation; The Second Tibetan Plateau Scientific Expedition and Research (STEP) Program, Grant/Award Number: 2019QZKK0503; US National Science Foundation, Grant/Award Number: DEB-0092642 and DEB-0445324

increased and were positively correlated with bacteriophage genes, suggesting a potential viral shunt in C degradation. In addition, eP increased the relative abundances of microbial stress tolerance genes, which are essential for coping with environmental stressors. Microbial responses to eP were phylogenetically conserved. The effects of eP on soil total C, root production, and microbes were interactively affected by eCO_2. Collectively, we demonstrate that long-term eP induces soil C loss, owing to changes in microbial community composition, functional traits, root production, and soil moisture. Our study unveils an important, previously unknown biosphere-climate feedback in Mediterranean-type water-limited ecosystems, namely how eP induces soil C loss via microbe-plant–soil interplay.

KEYWORDS
elevated precipitation, microbial functional trait, resource acquisition, soil carbon loss, viral shunt, water-limited ecosystems

1 | INTRODUCTION

The Anthropocene era has brought significant changes in Earth's precipitation patterns (Shaw et al., 2002). The global hydrologic cycle has intensified along with climate warming (Huntington, 2006), leading to an increase in annual precipitation in many regions during 1980–2019 (Gulev et al., 2021). Extreme precipitation events are anticipated to become more frequent in the 21st century (Corringham et al., 2019; Stevenson et al., 2022). As water availability serves as a limiting factor for most terrestrial ecosystems, the precipitation regime is a critical regulator of ecosystem functioning in soils, which comprise the Earth's largest terrestrial C reservoir (Reichstein et al., 2013). However, how precipitation regime shifts will affect soil C storage remains highly uncertain. To date, biogeochemical models have failed to reproduce precipitation-related patterns of soil C dynamics (Falloon et al., 2011), hampering our ability to predict how future scenarios of altered precipitation will influence soil C source or sink capacity.

The central west coast of North America, mainly in California, has a Mediterranean-type climate regime characterized by hot, dry summers, and cool, wet winters. The Jasper Ridge Global Change Experiment (JRGCE), which was conducted in a California annual grassland, demonstrated that net primary productivity (NPP) responded unimodally to variations in precipitation (Zhu et al., 2016). A short-term (3-year) elevated precipitation (eP) treatment increased NPP, primarily due to an increase in shoot production (Shaw et al., 2002). However, the positive shoot responses were largely offset by negative root responses, resulting in an insignificant increasing trend in total NPP over a 5-year eP treatment (Dukes et al., 2005). In addition, a study conducted in another California grassland revealed that long-term trajectories of plant species richness and abundances of invertebrate herbivores and predators differed from short-term responses to the eP treatment (Sullivan et al., 2016), suggesting that long-term eP treatment could restructure ecological relationships that ultimately affect soils and soil biota.

Soil microorganisms respond more rapidly to changes in soil water content than plants due to their faster intrinsic growth rates (Prosser et al., 2007). In a study of California grassland, soil active bacterial community examined by meta-transcriptomic analysis was rapidly affected by a wet-up event within 1–72 h, showing a consistent pattern conserved at the sub-phylum level (Placella et al., 2012). At the DNA level, wetting decreased the relative abundance of *Actinobacteria* but increased that of *Acidobacteria* (Barnard et al., 2013). However, these responses to short-term wetting were transient, displaying marked resilience. In contrast, fungal communities were largely unaffected, suggesting that fungi might be more resistant to changes in water availability. Furthermore, viral abundance in soils can be strongly influenced by water availability (Williamson et al., 2017).

Although numerous field experiments have explored the effect of short- or mid-term eP treatment on the taxonomic composition of microbial communities, the results have been

13652486, 2023, 18, Downloaded from https://onlinelibrary.wiley.com/doi/10.1111/gcb.16811 by University Of Oklahoma, Wiley Online Library on [21/09/2023]. See the Terms and Conditions (https://onlinelibrary.wiley.com/terms-and-conditions) on Wiley Online Library for rules of use; OA articles are governed by the applicable Creative Commons License

inconsistent: microbial community composition was affected by eP (3 years; Ochoa-Hueso et al., 2020), or not (2–8 years; Docherty et al., 2011; Gutknecht et al., 2012; Qi et al., 2021). In addition, the functional potentials of soil microbial communities, which underlie ecological processes, can be altered by eP. For instance, precipitation-mediated changes in microbial communities were strongly associated with increased soil respiration (Chou et al., 2008). Soil nitrifying and denitrifying enzyme activities, as well as the abundances of ammonia-oxidizing bacteria and nitrite-oxidizing bacteria, were also altered by the eP treatment in the JRGCE over 2–8 years since the experiment began (Barnard et al., 2006; Horz et al., 2004; Le Roux et al., 2016; Niboyet, Le Roux, et al., 2011). Increased soil N_2O emissions were reported under eP, which were associated with increased denitrification rates (Brown et al., 2012). Similarly, changes in the abundances and enzyme activities of soil denitrifiers were detected for a semi-arid grassland in response to precipitation-mediated changes (Shi et al., 2021).

Most studies examining soil microbial responses have focused on short-term eP treatments. It remains unclear whether microbial communities adapt to long-term altered soil moisture regimes as they do to elevated temperature (Melillo et al., 2017), or whether they continue to shift in the long-term trajectories to differ from short-term responses, as macrofauna and macroflora do (Sullivan et al., 2016). To address it, we examined plant and microbial responses (e.g., bacteria, fungi, and viruses) to a 14-year eP treatment (+50%) alone or combined with elevated CO_2 (eCO_2, +275 μmol mol^{-1}), warming (+1.0°C in topsoils) and nitrogen (N) deposition (+7 g m^{-2} $year^{-1}$) in the JRGCE, one of the longest manipulations of precipitation in a natural ecosystem. We hypothesized that long-term eP may lead to shifts in soil microbial community composition and functional traits, contradicting the short-term responses where eP affected microbial gene expression and physiology with no or transient changes in microbial community composition (Barnard et al., 2013; Gutknecht et al., 2012). We also hypothesized that the microbial responses to eP might be interactively affected by other climate change factors such as eCO_2, warming, and N deposition, as previously reported for plant production (Zhu et al., 2016).

2 | MATERIALS AND METHODS

2.1 | Experimental design and soil sampling

The JRGCE is located in an annual grassland within a 481-ha protected area along the eastern foothills of the Santa Cruz Mountains in northern California (37°40'N, 122°22'W). The mean annual precipitation at the study site over 45 years was 604 mm, with more than 80% of precipitation occurring as rain between November and March. The average annual air temperature over 45 years was 13.4°C. The soil is a fine-loamy, mixed, thermic Typic Haploxeralf, with a pH of 6.5–7.0 and a water-holding capacity of 21% (Brown et al., 2012).

The JRGCE was established in October 1998 to evaluate grassland ecosystem responses to global change treatments. The experiment consisted of eight blocks as replicates, each with four circular plots of 3.14 m^2 area. Each plot was equally divided into four quadrants, resulting in a total of 128 quadrants. To simulate the projected future precipitation regime in the California grassland, half of the quadrants received an additional 50% precipitation with sprinklers after each natural rainfall event, and two additional watering events in the spring at the end of the rainy season to simulate an extension of the rainy season by 3 weeks, while ambient precipitation (aP) quadrants received no water addition, serving as controls. During the 14 years of treatments preceding our study, ambient precipitation averaged 610 mm per year, and precipitation in the eP treatment averaged 870 mm (i.e., +42.6%, Figure S1a). In addition to elevated precipitation, the experiment included elevated carbon dioxide (ambient vs. +275 μmol mol^{-1} CO_2), warming (ambient vs. elevated temperature by ~1.0°C in topsoils), and N deposition (ambient vs. +7 g N m^{-2} $year^{-1}$ as $Ca(NO_3)_2$), all conducted in a full factorial design (Shaw et al., 2002). The treatments were arranged in a randomized block split-plot design, with warming and CO_2 elevation at the plot level and N deposition and eP assigned randomly at the subplot level (Dahlin et al., 2013; Gutknecht et al., 2012). In 2003, an accidental wildfire burned two of the eight blocks. In 2011, a controlled burn was carried out in half of the blocks, including the two blocks burned in 2003, to provide a fire treatment. Since previous studies found that fire significantly affected microbial communities and ecosystem functioning across four global change treatments (Niboyet, Brown, et al., 2011; Strong et al., 2017; Yang et al., 2020), the burned blocks were excluded from the present analysis.

A total of 64 soil samples were collected on April 26 and 27, 2012, 14 years after the initial treatments were implemented. Soil samples were obtained by collecting one 7 cm deep × 5 cm diameter core from each quadrant and thoroughly homogenizing the soil. These soil samples were then sieved through a 2 mm mesh and stored at −20°C for geochemical analyses or at −80°C for microbial analyses.

2.2 | Environmental variables

We determined soil total C and total N by combustion analysis on a Carlo Erba Model 1500 CNS Analyzer (Carlo Erba Strumentazione). Soil C:N ratios were then calculated as mass ratios of total C to total N. We also collected soil total C and N data in 1998 (Year 0) and from 2000 (Year 2) to 2012 (Year 14) on a yearly basis. To measure soil temperature, we buried thermo-couples at a depth of 2 cm in each quadrant and recorded hourly data, which we then averaged over April 1–27, 2012 (Niboyet, Le Roux, et al., 2011). We determined soil moisture by comparing the mass of a 10-g soil sub-sample before and after drying at 105°C for 1 week. We measured soil pH by suspending 5 g of soil in 10 mL of distilled water. We determined soil ammonium (NH_4-N) and nitrate (NO_3-N) concentrations by suspending 5 g of soil in 50 mL of 2 M KCl solution, followed by measuring filtered extracts using an Automated Segmented Flow Analyzer

13652486, 2023, 18, Downloaded from https://onlinelibrary.wiley.com/doi/10.1111/gcb.16811 by University Of Oklahoma, Wiley Online Library on [21/09/2023]. See the Terms and Conditions (https://onlinelibrary.wiley.com/terms-and-conditions) on Wiley Online Library for rules of use; OA articles are governed by the applicable Creative Commons License

(SEAL Analytical). We collected soil CO_2 efflux data as previously described (Strong et al., 2017), which were measured from April 27–29 to June 20–25, 2012.

The ecosystem NPP and its components, that is, aboveground NPP (ANPP) and belowground NPP (BNPP) were measured as previously described (Zhu et al., 2016). Specifically, we collected aboveground plant materials from a 141 cm^2 area of each quadrant twice at the peak of standing biomass, once in mid-April to early May and again in early to late May. The biomass was analyzed using a maximum of two harvests to reduce phenological variation bias under different treatments. We measured the total aboveground biomass by clipping all aboveground biomass, separating individual plant species into functional groups: annual grass, perennial grass, annual forb, and perennial forb (Gao et al., 2021). We determined litter biomass by collecting all senesced plant material from the ground within the same area. After the first aboveground harvest, we determined belowground biomass by taking four soil cores (2.5 cm diameter) in the same area, with two cores for shallow roots (0–15 cm) and two for deep roots (15–30 cm). Fine roots in a depth of 0–15 cm were separated from tap roots. All plant materials were oven-dried at 70°C and weighed. NPP, ANPP, and BNPP data in 1998 and from 2000 to 2011 (BNPP and NPP in 1999 and 2007 not available) were also collected as previously described (Zhu et al., 2016).

2.3 | DNA extraction, purification and quantification

We extracted soil DNA by freeze-grinding mechanical lysis, as previously described (Zhou et al., 1996). We purified DNA with a 0.5% low-melting-point agarose gel electrophoresis followed by phenol-chloroform-butanol extraction. We assessed DNA quality using absorbance ratios of 260/280 nm and 260/230 nm (260/280 > 1.8 and 260/230 > 1.7) with a NanoDrop ND-1000 Spectrophotometer (NanoDrop Technologies). We then quantified the final DNA concentration with a PicoGreen method, using an FLUO star Optima (BMG Labtech) as previously described (Yang et al., 2014).

2.4 | MiSeq sequencing and raw data preprocessing

We constructed the 16S rRNA gene library and processed sequencing data as previously described (Guo et al., 2019). We targeted the V4 region of the 16S rRNA gene with primers 515F (GTGCCAGCMGCCGCGGTAA) and 806R (GGACTACHVGGGTWTCTAAT) and ITS2 region between 5.8S and 28S rRNA genes with primers gITS7 (GTGARTCATCGARTCTTTG) and ITS4 (TCCTCCGCTTATTGATATGC) in PCR amplification. We then sequenced PCR products by 2 × 250 bp paired-end sequencing with a MiSeq instrument (Illumina). We identified paired-end raw sequences by paired barcodes and combined them using FLASH (Magoč & Salzberg, 2011). We further trimmed sequences to the length of >245 bp for the 16S rRNA gene or >220 bp for the ITS. We generated amplicon sequence variants (ASVs), also known as zero-radius operational taxonomic units or unique sequence variants, by UNOISE3 (Edgar, 2018). We annotated the representative sequence taxonomy using the QIIME2 Naive Bayes classifier trained for the V4 region of the 16S rRNA gene (version Silva-132-99-515-806) and ITS based on UNITE QIIME release (version ver8_97_10.05.2021; Abarenkov et al., 2021; Quast et al., 2013). We removed the singlet ASVs and those classified as mitochondria and chloroplasts to improve data reliability. We retrieved 3,391,680 high-quality sequences for the 16S rRNA gene and 661,632 high-quality sequences for ITS. Then, we resampled 16S rRNA gene sequences at a depth of 31,441 reads and ITS sequences at a depth of 17,397 reads for each of the 64 samples (Figure S2). The representative 16S rRNA gene sequences were aligned using MAFFT and used for constructing phylogenetic trees by FastTree on QIIME2 (Bolyen et al., 2019). Although the ITS2 region has a high resolution for identifying evolutionarily close taxa, the high rate of insertion and deletion makes the evolutionarily distant taxa vary greatly and difficult to be aligned. Therefore, we constructed the fungal phylogenetic tree by specifying constraint alignment in FastTree v2.1.10 (Price et al., 2010). The constraint alignment was converted from a guide tree constructed using ghost-tree (Fouquier et al., 2016), which grafted the taxonomically assigned ITS sequences to a reference foundation tree (Silva Ver. SSU 138) by mapping genus names.

2.5 | GeoChip experiments and raw data preprocessing

We carried out DNA labeling with Cy3 and hybridization with the functional array GeoChip 4.6, as previously described (Wang et al., 2018). We scanned the fluorescent intensities of each probe on GeoChip, using a NimbleGen MS 200 Microarray Scanner with 100% laser power and 100% photomultiplier tube (Roche). We discarded spots with a signal-to-noise ratio of less than 2.0. Probe signals that were detected only once among four biological replicates were also excluded. As a result, a total of 60,619 probes, including 53,748 probes derived from bacteria, 4661 probes from eukaryotes, 1821 probes from archaea, and 389 from viruses, were detected. We performed a natural logarithmic transformation of each detected probe (a_{ij}) (probe $j \in [1, 60{,}619]$, sample $i \in [1, 64]$) to get $b_{ij} = \ln(a_{ij} + 1)$ (we added 1 to a_{ij} because the natural logarithm of zero is not defined). We normalized b_{ij} by dividing the average signal intensity of all probes in the sample i to get $c_{ij} = b_{ij} / \mathrm{Avg}_{j=1}^{m} b_{ij}$ (m is the total number of probes, i.e., 60,619).

2.6 | Statistical analyses

All statistical analyses were performed in R version 3.5.2 (http://www.r-project.org) unless otherwise specified. p-values <.050 are

13652486, 2023, 18, Downloaded from https://onlinelibrary.wiley.com/doi/10.1111/gcb.16811 by University Of Oklahoma, Wiley Online Library on [21/09/2023]. See the Terms and Conditions (https://onlinelibrary.wiley.com/terms-and-conditions) on Wiley Online Library for rules of use; OA articles are governed by the applicable Creative Commons License

considered to be statistically significant. *p*-values between .050 and .100 are considered to be marginally significant, given the large variations among blocks. *p*-values >.100 are not considered to be statistically significant.

2.6.1 | Diversity analyses

We calculated the α-diversity of the Shannon index for taxonomic diversity (based on rarefied ASV tables) and functional gene diversity (based on functional genes of GeoChip), and Faith's phylogenetic diversity. We utilized the vegan and picante packages for these analyses.

2.6.2 | Treatment effect analyses

To assess the treatment effect, we calculated the effect size of precipitation as follows: % effect = 100% × (eP−aP)/aP ($n = 64$ under eP and aP for data in 1998 and 2000–2003 before the 2003 fire, $n = 48$ for data in 2004–2011 before the 2011 fire, and $n = 32$ for data in 2012). The statistical significance of the treatment effect was tested by split-plot ANOVA using aov function in R. We applied log or square root transformations to improve normality when necessary. To analyze the treatment effect on functional and taxonomic compositions of microbial communities, we performed split-plot PERMANOVA with PRIMER 6 + PERMANOVA software (Marti et al., 2008). We used negative binomial models in the DESeq2 package to identify significantly changed ASVs with eP (baseMean >10, log2 fold change >0.5, and FDR adjusted $p < .050$), and examined the significance with Wald tests (Love et al., 2014). Using DESeq2 and split-plot ANOVA, we also examined the effects of the eP treatment across different taxonomic levels to determine whether the alterations in taxonomic lineages were phylogenetically clustered. We adjusted *p*-values using the FDR method when conducting multiple comparisons, such as assessing the eP effect on multiple functional genes and taxonomic lineages.

2.6.3 | ConsenTRAIT analysis

We performed consenTRAIT analysis to determine whether the responses of bacteria and fungi to eP were phylogenetically conserved, using the castor package (Louca & Doebeli, 2018; Martiny et al., 2013). Since FastTree only estimates branch lengths by inferring approximately-maximum-likelihood phylogenetic trees, we constructed a maximum likelihood (ML) tree of the 16S rRNA gene sequences to obtain accurate branch lengths for the consenTRAIT analysis. For ITS sequences, it is difficult to align the sequences and construct an ML tree because of high variations, we constructed the phylogenetic tree using constrained FastTree's topology search instead.

2.6.4 | Ecological process analyses

Microbial community assemblies are shaped by ecological processes, including both stochastic processes (e.g., dispersal, birth-death events, and ecology drift) and deterministic processes (e.g., environmental filtering; Hubbell, 2001; Ning et al., 2019). We estimated the stochastic ratio using a modified method based on null-model algorithms with taxonomic metrics (Sorensen) as previously described (Guo et al., 2018; Ning et al., 2019). The effect of the eP treatment on the estimated stochastic ratio was evaluated by split-plot permutational multivariate analysis of variance (PERMANOVA).

2.6.5 | Structural equation modeling and aggregated boosted tree analyses

Structural equation modeling (SEM) was employed to reveal how biotic and abiotic variables affect soil total C across aP and eP quadrants. Since soil total C was altered by both eP and N deposition (Table S1), only samples under the ambient N condition (a total of 32 samples) were used for SEM analysis to exclude the effect of N deposition. The community compositions were represented by PC1 from the principal coordinate analysis based on the Bray–Curtis dissimilarity of the ASV matrix, which captured 9.3%–15.5% variations of microbial community composition. We first established a full model with all reasonable pathways (Figure S3), and then we used a stepwise approach to remove non-significant pathways with the highest *p*-value at each step until the final model was obtained. The SEM analysis was performed using the lavaan R package (Rosseel, 2012).

We performed the aggregated boosted tree (ABT) analysis, a machine learning algorithm, to investigate the relative influences of biotic and abiotic variables in regulating soil total C (De'ath, 2007). We first established a hyper grid of parameters, including learning rate (shrinkage), interaction depth, the minimum number of observations in the terminal nodes of trees (n.minobsinnode), and subsampling fraction (bag.fraction), for tree training and tuning (Data S1). However, when shrinkage was set to 0.001, the optimal trees became too large, which might lead to overfitting of the ABT models. Therefore, we opted for the optimal combination of parameters, which included shrinkage = 0.01, interaction depth = 1, n.minobsinnode = 3, and bag.fraction = 0.8. Finally, we evaluated the model by 10-fold cross-validation. ABT models were built by gbm function in gbm R package, and model evaluation was performed by train function in caret R package.

3 | RESULTS

3.1 | Edaphic and plant variables

The eP treatment did not change soil total C in the early phase of the 2nd–9th year since the experiment began (Figure 1a and Table S2). In the late phase of the 10th–14th year, eP decreased soil total C by

13652486, 2023, 18, Downloaded from https://onlinelibrary.wiley.com/doi/10.1111/gcb.16811 by University Of Oklahoma, Wiley Online Library on [21/09/2023]. See the Terms and Conditions (https://onlinelibrary.wiley.com/terms-and-conditions) on Wiley Online Library for rules of use; OA articles are governed by the applicable Creative Commons License

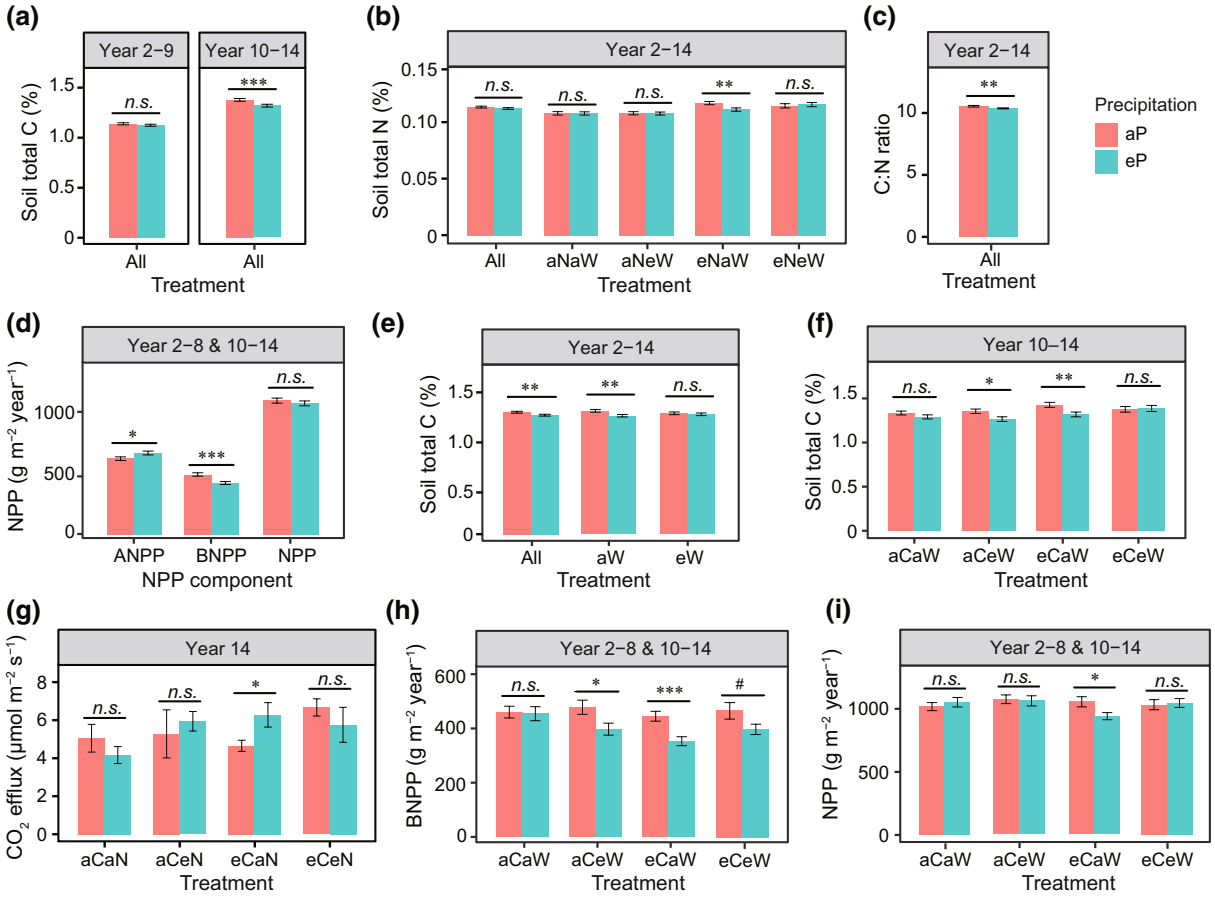

FIGURE 1 The effects of the eP treatment on soil total C, soil total N, CO_2 efflux, and plant variables in the 2nd–14th year after the experiment treatment began. (a) Soil total C in phase I over the 2nd–9th years and in phase II over the 10th–14th years. (b) Soil total N. (c), Soil C:N ratio, calculated as the mass ratio of soil total C to N. (d) ANPP, BNPP, and NPP. As BNPP in the 9th year was not measured, only data in Years 2nd–8th and 10th–14th are displayed. (e) Soil total C under different warming treatments. (f) Soil total C in phase II over 10th–14th years under different CO_2 and warming treatments. (g) Soil CO_2 efflux in the 14th year. (h) BNPP under different CO_2 and warming treatments. (i) NPP under different CO_2 and warming treatments. Means and standard errors are indicated. Treatments: all, across other climate change factors; aC, ambient CO_2; eC, elevated CO_2; aW, ambient temperature, eW, warming; aN, ambient N; eN, N deposition. $^{***}p<.001$, $^{**}p<.010$, $^{*}p<.050$, and $^{\#}p<.100$. BNPP, belowground NPP; NPP, net primary productivity. [Colour figure can be viewed at wileyonlinelibrary.com]

4.2% ($p<.001$, Figure 1a and Table S2), with significant eP effects on soil total C in the 10th, 13th, and 14th year ($p<.021$, Figure S1b). Soil total N was not altered by eP alone (Figure 1b and Table S2). As a result, the C:N ratio was significantly decreased by eP ($p=.002$, Figure 1c and Table S2). Treatment effects on other soil variables were described in Supplementary Text A.

Aboveground net primary production (ANPP) was increased from 591 g m^{-2} $year^{-1}$ in ambient precipitation (aP) quadrants to 632 g m^{-2} $year^{-1}$ in eP quadrants throughout the 2nd–14th year ($p=.018$, Figure 1d and Table S2). In contrast, BNPP was decreased from 463 g m^{-2} $year^{-1}$ in aP quadrants to 401 g m^{-2} $year^{-1}$ in eP quadrants ($p<.001$, Figure 1d and Table S2). The decline in BNPP counterbalanced the increase in ANPP, resulting in an unchanged NPP by the eP treatment (Figure 1d). However, eP effects on ANPP and BNPP varied considerably by year (Figure S1c,d). ANPP was significantly increased in only 2 years of the 14-year observations (Figure S1c), while BNPP was significantly decreased by 14.9%–25.2% during the first 2nd–5th years ($p<.021$, Figure S1d). However, the decline in BNPP was only observed in 3 years during the late 6th–14th years (Figure S1d).

There was an interactive effect of precipitation×warming on soil total C ($p=.048$, Table S2), which was decreased by eP when the temperature was ambient but was unaltered by eP when the temperature was elevated (Figure 1e). In the early phase of the 2nd–9th year, soil total C was not altered by eP alone or combined with other global change factors (Table S2). In contrast, soil total C was interactively affected by precipitation×CO_2×warming in the late phase of the 10th–14th year ($p=.008$, Table S2), leading to a decline in soil total C under eP when CO_2 or temperature was elevated (Figure 1f). Soil CO_2 efflux was measured in the 14th year of the experiment. Soil CO_2 efflux was interactively affected by precipitation×CO_2×N deposition ($p=.022$, Table S3), with eP increasing CO_2 efflux when CO_2 was elevated and N was ambient (Figure 1g). Soil total N was interactively affected by precipitation×N deposition×warming ($p=.047$, Table S2), with eP decreasing soil total N only under N deposition and ambient temperature (Figure 1b). BNPP and NPP were interactively affected by precipitation×CO_2×warming

13652486, 2023, 18, Downloaded from https://onlinelibrary.wiley.com/doi/10.1111/gcb.16811 by University Of Oklahoma, Wiley Online Library on [21/09/2023]. See the Terms and Conditions (https://onlinelibrary.wiley.com/terms-and-conditions) on Wiley Online Library for rules of use; OA articles are governed by the applicable Creative Commons License

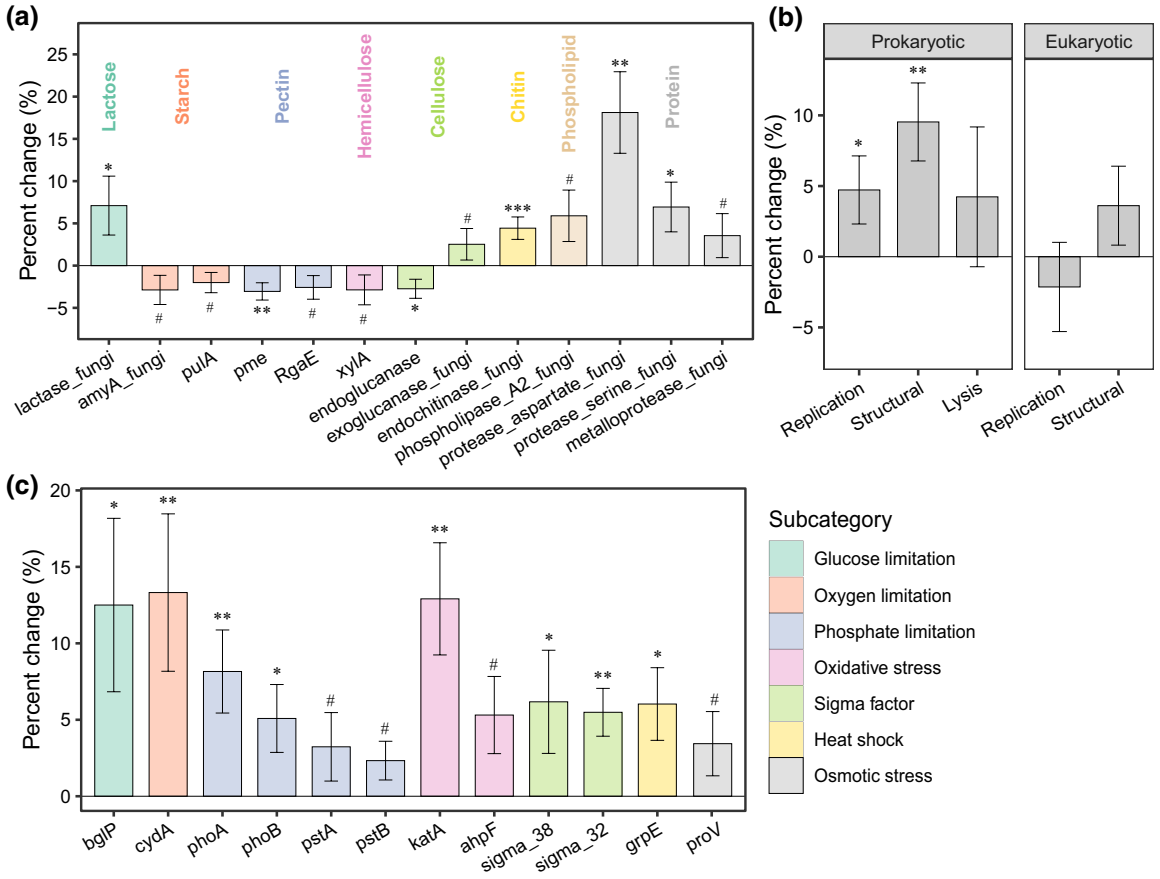

FIGURE 2 The effects of the long-term eP treatment on C degradation genes, viral genes, and stress response genes. (a) Percent changes of individual C degradation genes. Labels represent targeted substrates. The percent change represents the effect size of relative abundances calculated as follows: % effect = 100% × (eP−aP)/aP. (b) Percent changes of functional subcategories for prokaryotic and eukaryotic viral genes. (c) Percent changes of individual stress response genes. Only significantly and marginally significantly changed genes (FDR corrected $p < .100$) are shown. The error bar represents the standard error ($n = 32$). $^{***}p < .001$, $^{**}p < .010$, $^{*}p < .050$, and $^{\#}p < .100$. [Colour figure can be viewed at wileyonlinelibrary.com]

($p < .037$, Table S2), with eP decreasing BNPP when CO_2 and temperature were elevated (Figure 1h) and decreasing NPP when CO_2 was elevated and the temperature was ambient (Figure 1i).

3.2 | Microbial functional genes

To examine the shifts in microbial communities by long-term eP, we analyzed microbial functional potentials with functional gene array (GeoChip 4.6) and prokaryotic and fungal community compositions with targeted amplicon sequencing, using soil samples collected in the 14th year of the experiment. Microbial functional gene composition differed between the aP and eP quadrants ($p = .050$, Table S4), though functional gene α-diversity remained similar (Table S5). There were interactive effects of precipitation × CO_2 on functional gene composition and α-diversity (Tables S4 and S5). Functional gene α-diversity increased with eP when CO_2 was elevated, while it was not affected by eP when CO_2 was ambient (Figure S4).

The relative abundances of genes associated with the degradation of pectin (*pme*) and cellulose (the gene encoding endoglucanase derived from bacteria) were decreased in the eP quadrants ($p < .025$, Figure 2a). In contrast, the relative abundances of fungal genes encoding enzymes related to the degradation of N-rich compounds, such as chitin (endochitinase) and protein (aspartate protease and serine protease), were increased by 4.4%–18.1% with eP ($p < .025$, Figure 2a). In addition, the relative abundance of the marker gene for methanogenesis (*mcrA*) increased ($p = .017$) under eP, while those of methane oxidation genes *mmoX* and *pmoA* were unaltered (Figure S5a). There were interactive effects of precipitation × CO_2 on C degradation genes, but not methane cycling genes (Data S2). Notably, the increase in relative abundances of genes associated with degrading N-rich compounds was greater when CO_2 was elevated (Figure S6a). Taken together, these results suggest that eP substantially altered soil microbial C cycling potentials, especially when CO_2 was elevated.

Since bacteriophages play an important role in regulating microbial C dynamics, we investigated 221 bacteriophage genes detected in our samples. The relative abundances of bacteriophage genes associated with viral structure and replication increased by 4.7%–9.5% in eP quadrants ($p < .040$, Figure 2b), suggesting that eP may stimulate bacteriophage growth. In contrast, the total abundances of 101 eukaryotic viral genes detected in our samples remained unaltered (Figure 2b). There were interactive effects of precipitation × CO_2 on bacteriophage genes (Data S2), whose gene abundances increased with eP when CO_2 was elevated (Figure S6b).

13652486, 2023, 18, Downloaded from https://onlinelibrary.wiley.com/doi/10.1111/gcb.16811 by University Of Oklahoma, Wiley Online Library on [21/09/2023]. See the Terms and Conditions (https://onlinelibrary.wiley.com/terms-and-conditions) on Wiley Online Library for rules of use; OA articles are governed by the applicable Creative Commons License

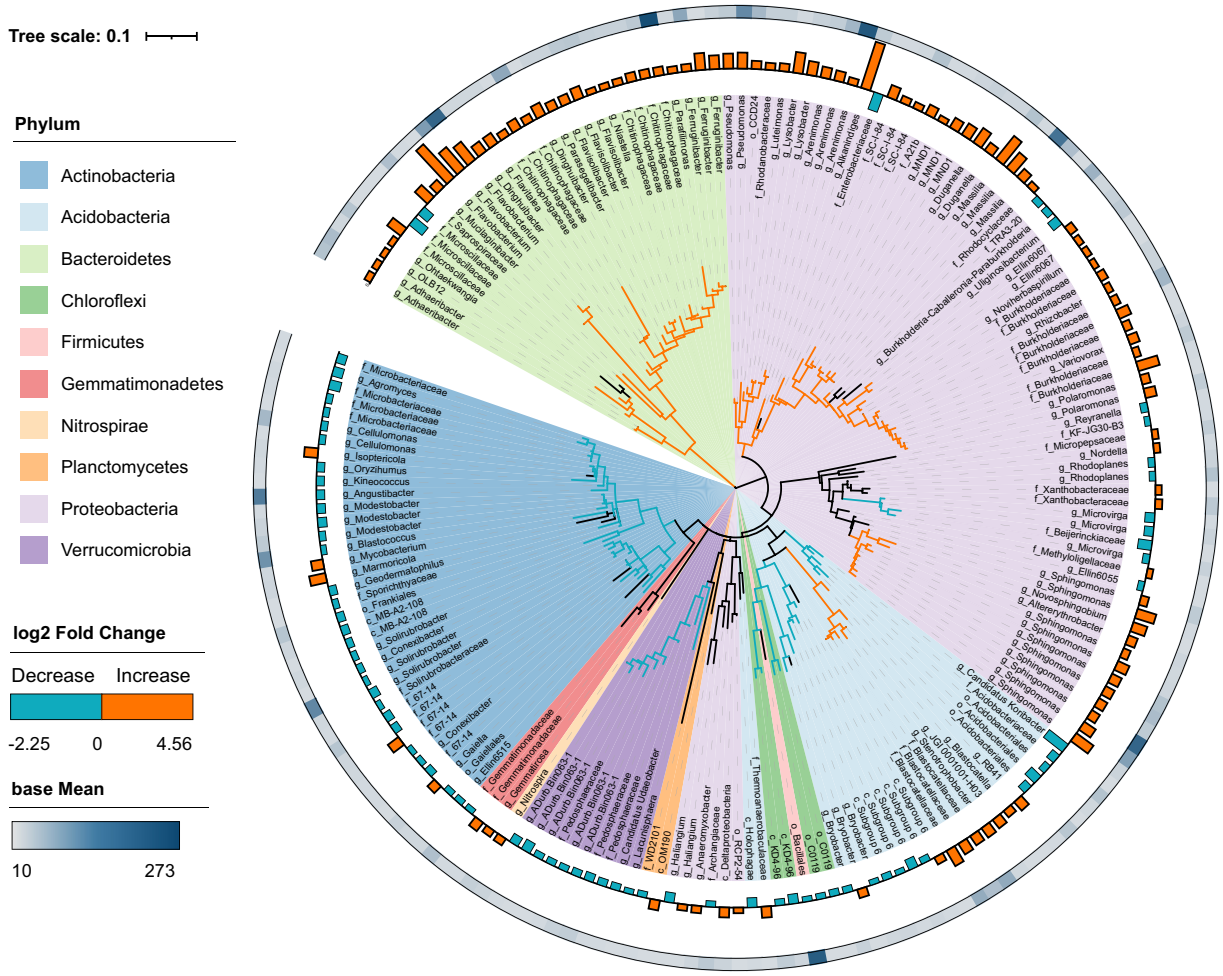

FIGURE 3 The phylogenetic tree of bacterial ASVs significantly changed by eP. The inner colored ring represents the phylum of each ASV. The middle ring of colored bars represents the relative $\log_2$-fold change of each ASV in eP quadrants compared with aP quadrants. The outer ring displays the mean relative abundance of each ASV. The colored branches represent the phylogenetically clustered groups (families and higher taxonomic level clades), with orange branches indicating increased groups and blue-green branches indicating decreased groups. [Colour figure can be viewed at wileyonlinelibrary.com]

Since long-term eP decreased soil total C, we investigated whether microbial stress responses were stimulated. The relative abundances of eight stress response genes were significantly increased with eP (Figure 2c), including those associated with glucose limitation, oxygen limitation, phosphate limitation, oxidative stress, and sigma factors (see Supplementary Text B for details). There were interactive effects of precipitation × CO_2 on phosphate limitation and sigma factor genes (Data S2), whose gene abundances increased with eP when CO_2 was elevated and the temperature was ambient (Figure S6c,d).

TABLE 1 The consenTRAIT analysis showing phylogenetic conservation of microbial responses to eP.

Kingdom	Response	τ_D [a]	*p*-value [b]
Bacteria	Increase	0.116	**<.001**
	Decrease	0.063	**<.001**
Fungi	Increase	0.190	.211
	Decrease	0.267	**.004**

[a] τ_D is the mean phylogenetic depth at which the response is conserved across clades.

[b] Significance values were estimated using 999 randomizations ($p < .050$ in bold). A significant value indicates a greater mean depth than randomization, indicating deeper-rooting conservation across clades.

3.3 | Microbial taxonomic composition

We identified 4649 to 14,940 prokaryotic ASVs and 719 to 1757 fungal ASVs per sample (Figure S2). Their taxonomic compositions were different between the eP and aP quadrants ($p = .001$) but were barely affected by the interaction of precipitation and other climate change treatments (Table S4). The taxonomic and phylogenetic α-diversities remained unaltered between the eP and aP quadrants (Table S5).

Positive eP responders of bacteria, that is, bacterial ASVs increased by eP, were clustered within *Bacteroidetes*, *Gammaproteobacteria*, the order *Sphingomonadales* of

13652486, 2023, 18, Downloaded from https://onlinelibrary.wiley.com/doi/10.1111/gcb.16811 by University Of Oklahoma, Wiley Online Library on [21/09/2023]. See the Terms and Conditions (https://onlinelibrary.wiley.com/terms-and-conditions) on Wiley Online Library for rules of use; OA articles are governed by the applicable Creative Commons License

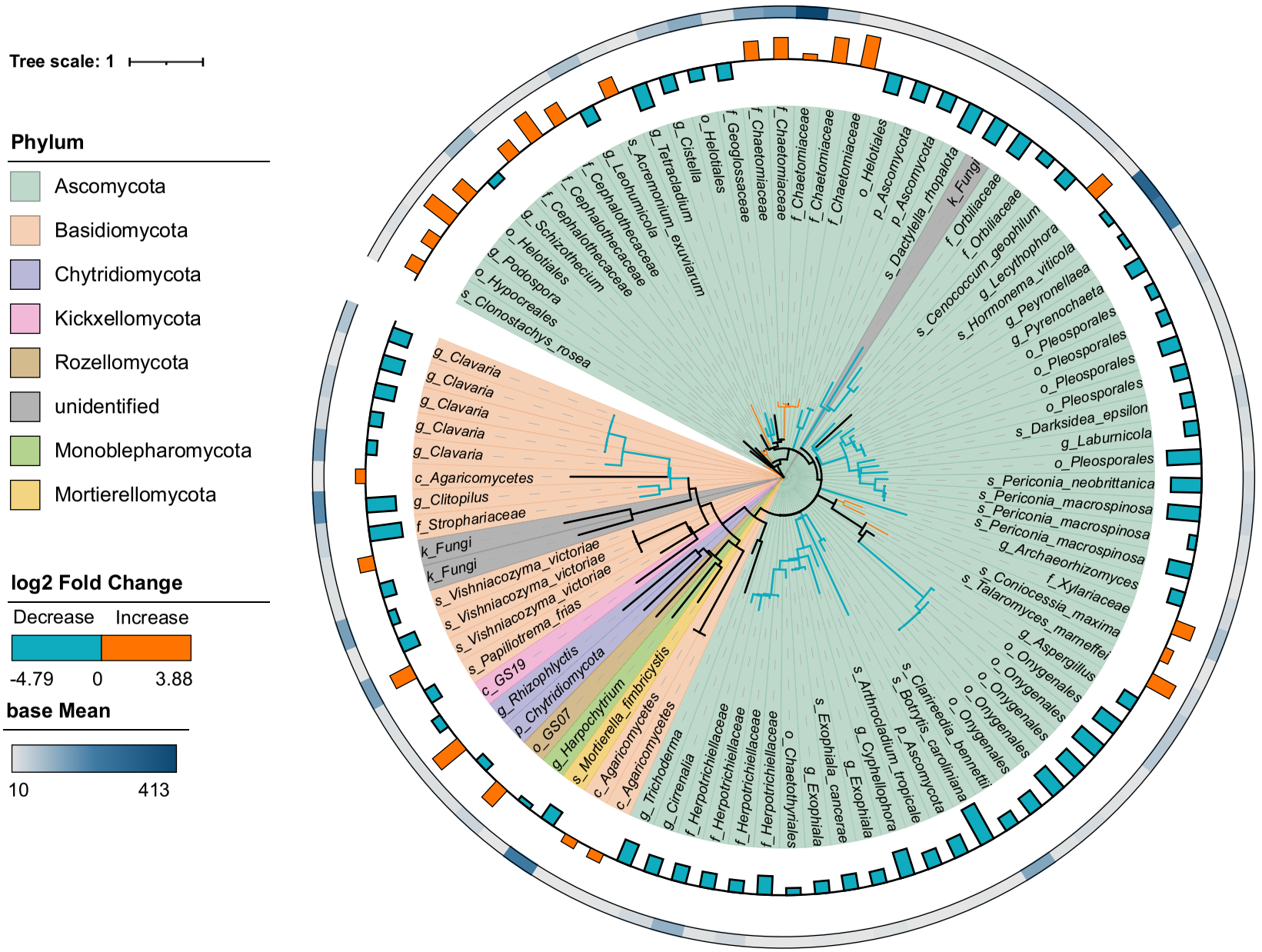

FIGURE 4 The phylogenetic tree of fungal ASVs significantly changed by eP. The inner colored ring represents the phylum of each ASV. The middle ring of colored bars represents the relative $\log_2$-fold change of each ASV in eP quadrants compared with aP quadrants. The outer ring indicates the mean relative abundance of each ASV. The colored branches represent the phylogenetically clustered groups (families and higher taxonomic level clades), with orange branches indicating increased groups and blue-green branches indicating decreased groups. [Colour figure can be viewed at wileyonlinelibrary.com]

13652486, 2023, 18, Downloaded from https://onlinelibrary.wiley.com/doi/10.1111/gcb.16811 by University Of Oklahoma, Wiley Online Library on [21/09/2023]. See the Terms and Conditions (https://onlinelibrary.wiley.com/terms-and-conditions) on Wiley Online Library for rules of use; OA articles are governed by the applicable Creative Commons License

Alphaproteobacteria, and the order *Blastocatellales* of *Acidobacteria* (Figure 3 and Data S3, see Supplementary Text C for details). Negative eP responders of bacteria, that is, bacterial ASVs decreased by eP, were clustered within *Actinobacteria*, *Verrucomicrobia*, *Chloroflexi*, subgroup6 of *Acidobacteria*, and the family *Beijerinckiaceae* of *Alphaproteobacteria* (Figure 3 and Data S3). The positive and negative eP responders were phylogenetically clustered in these clades at a greater depth than expected in a null model of consenTRAIT analysis ($p < .001$, Table 1), suggesting that the bacterial community's response to long-term eP was phylogenetically conserved.

Positive eP responders of fungi were clustered within the class *Sordariomycetes* and the order *Eurotiales* of *Ascomycota* (Figure 4 and Data S4). Negative eP responders of fungi were clustered in the class *Archaeorhizomycetes*, the order *Onygenales*, *Helotiales*, and *Orbiliales*, the family *Periconiaceae* and *Herpotrichiellaceae* of *Ascomycota*, and the order *Agaricales* of *Basidiomycota* (Figure 4 and Data S4). The negative eP responders of fungi were phylogenetically conserved in deep-rooting clades ($p = .003$), however, the positive eP responders were not, as indicated by the absence of significant phylogenetic conservation (Table 1).

3.4 | Ecological processes in shaping microbial community assembly

The phylogenetically conserved response of microbial communities to eP implies that environmental filtering, a deterministic process, may be important under eP. To test this, we estimated the relative importance of stochastic and deterministic processes using a null model analysis. There were interactive effects of precipitation × CO_2 on the stochastic ratios of bacterial communities ($p = .004$), which decreased with eP when CO_2 was elevated ($p = .031$) but remained unaltered with eP when CO_2 was ambient (Figure 5a). In contrast, stochastic ratios of fungal community decreased with eP regardless of CO_2 conditions (Figure 5b), showing higher environmental selection.

To identify the deterministic factors that affect microbial community composition, we conducted Mantel tests to examine the linkages between environmental variables and microbial eP responders. The positive eP responders of fungi and negative eP responders of bacteria were both correlated with soil moisture and soil CO_2 efflux (Mantel's $r = .149–.203$, $p < .015$, Figure 5c). In contrast, the negative eP responders of fungi and positive eP responders of bacteria were correlated with environmental variables to a lesser degree (see

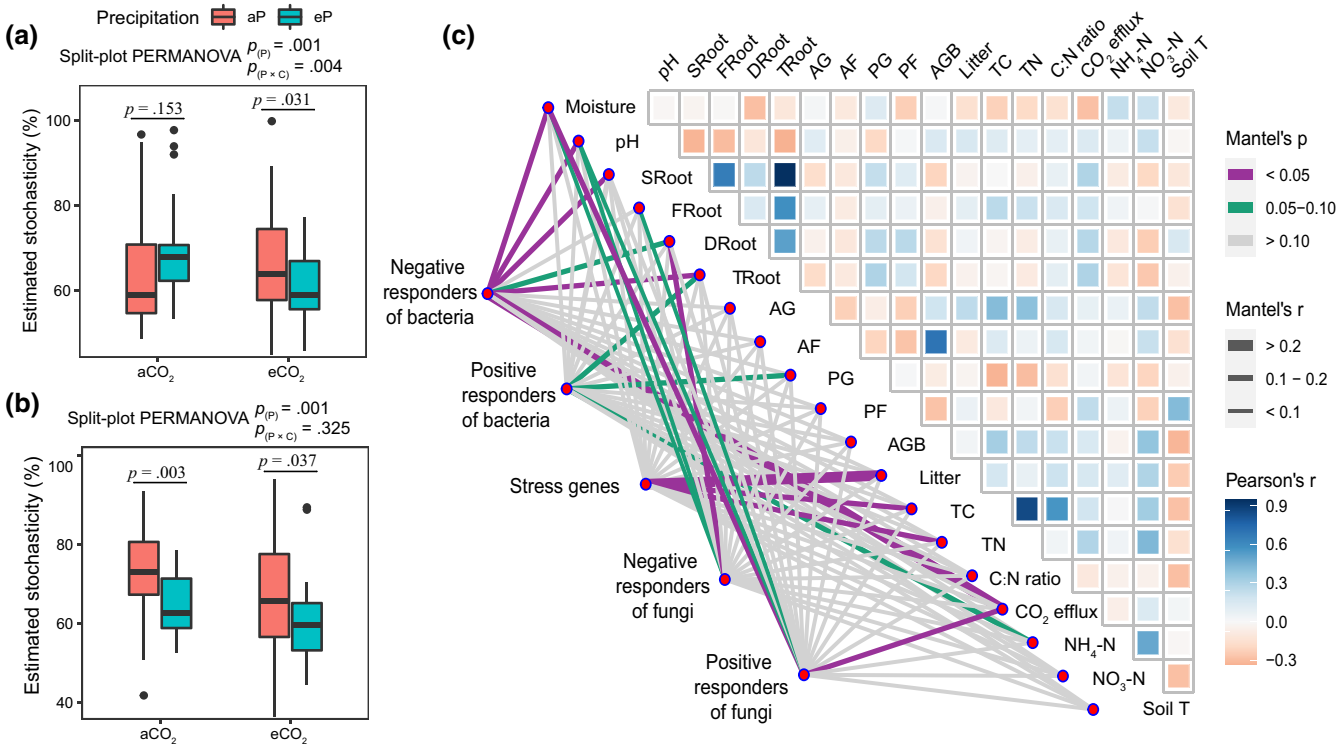

FIGURE 5 Stochastic and deterministic factors influencing microbial communities. (a) The estimated stochastic ratio in prokaryotic community assembly. The significance of the effect for each treatment was tested by split-plot PERMANOVA. P: precipitation, C: CO_2. The significance of the eP treatment under different CO_2 regimes was tested by *t*-test. (b) The estimated stochastic ratio in fungal community assembly. (c) Environmental variables driving composition changes of ASVs and stress genes significantly altered by the eP treatment. The color gradient represents Pearson's correlation coefficients of pairwise correlations of environmental variables. The edge width corresponds to the Mantel correlation coefficients, and the edge color denotes the statistical significance of the Mantel tests. SRoot, shallow root biomass (0–15 cm); FRoot, fine root biomass (0–15 cm); DRoot, deep root biomass (15–30 cm); TRoot, total root biomass; AG, annual grass biomass; AF, annual forb biomass; PG, perennial grass biomass; PF, perennial forb biomass; AGB, aboveground biomass; TC, soil total C; TN, soil total N; Soil T, soil temperature. [Colour figure can be viewed at wileyonlinelibrary.com]

13652486, 2023, 18, Downloaded from https://onlinelibrary.wiley.com/doi/10.1111/gcb.16811 by University Of Oklahoma, Wiley Online Library on [21/09/2023]. See the Terms and Conditions (https://onlinelibrary.wiley.com/terms-and-conditions) on Wiley Online Library for rules of use; OA articles are governed by the applicable Creative Commons License

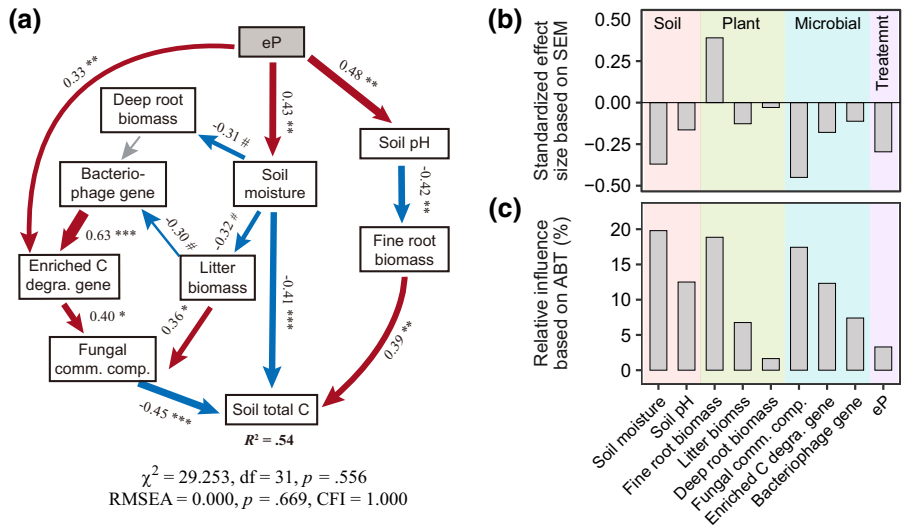

FIGURE 6 Biotic and abiotic drivers in regulating soil total C content. (a) The structural equation model (SEM) showing the influences of the eP treatment (grey rectangle), environmental variables and microbial profiles on soil total C. Red arrows represent significant and marginally significant positive pathways, and blue arrows represent significant and marginally significant negative pathways. The width of each arrow is proportional to the strength of the relationship and numbers near the pathway represent the standardized path coefficients. Bootstrap-based *p*-values for path coefficients are indicated by ***when $p < .001$, **when $p < .010$, *when $p < .050$, and #when $p < .100$. R^2 represents the proportion of variance explained for soil total C. (b) Standardized total effects (direct and indirect effects) based on SEM. (c), The relative influences of biotic and abiotic variables in affecting soil total C, as revealed by aggregated boosted tree (ABT) analysis. Enriched C degra. gene represents the relative abundances of increased C degradation genes shown in Figure 2a, including those in the degradation of chitin and protein. Fungal comm. comp. refers to fungal community composition, as represented by the PC1 from the principal coordinate analysis based on the Bray-Curtis distance of the fungal ASV matrix. [Colour figure can be viewed at wileyonlinelibrary.com]

Supplementary Text D for details). We also examined the linkages between environmental variables and stress response genes and found that stress response genes were correlated with soil total C, soil total N, and litter biomass (Mantel's $r = .101–.267$, $p < .050$, Figure 5c).

3.5 | Biotic and abiotic variables linking to soil total C

Since soil total C decreased with long-term eP, we identified biotic and abiotic variables that could be major drivers of soil total C. SEM analyses were performed with the presumed relationships (Figure S3) among the selected subsets of edaphic and plant variables that were least correlated (see Section 2 for details of model selection). Soil total C was negatively affected by soil moisture but positively affected by fine root biomass (Figure 6a). Soil total C was significantly correlated with fungal community composition, which was, in turn, correlated with relative abundances of genes associated with the degradation of N-rich chitin and protein. The relative abundances of bacteriophage genes had a strong correlation with those of C degradation genes, likely revealing an important role of viral shunt on soil C cycling. Overall, these variables explain 54% of the variations in soil total C (Figure 6a). Among all the tested independent variables, soil moisture, fine root biomass, and fungal community composition played essential roles in mediating soil total C, as revealed by both SEM and ABT analysis (Figure 6a,b). Soil pH and enriched microbial C degradation genes influenced soil total C to lesser extents. These results indicate that soil, plant, and microbial variables explain a similar proportion of soil total C dynamics.

4 | DISCUSSION

Understanding how long-term climate changes affect soil microbial communities and underlying ecosystem processes is essential for better predicting the terrestrial responses to climate change (Tiedje et al., 2022). By examining the effects of 14-years eP on edaphic variables, plants, bacteria, fungi, and viruses, our study provides explicit evidence that long-term eP, either alone or in combination with other climate change drivers, can alter ecosystem compositions and functional traits linked to soil C loss.

4.1 | The long-term eP treatment shifts microbial community compositions and functional traits

Although the short- or mid-term (3–8 years) eP treatment in the JRGCE did not alter microbial community composition (Docherty et al., 2011; Gutknecht et al., 2012), we found that bacterial and fungal community compositions were significantly changed after 14-year eP treatment (Table S4). This result supports our hypothesis that microbial communities continue to shift in the long-term trajectories, differing from short-term responses (Sullivan et al., 2016). However, this discrepancy could also be attributed to technical differences. Previous studies, which relied on low-resolution microbial community fingerprinting based on lipid biomarker analysis, may not unveil variations in microbial community composition (Docherty et al., 2011; Gutknecht et al., 2012). Our analysis offers supporting evidence that microbial responses to water availability

13652486, 2023, 18, Downloaded from https://onlinelibrary.wiley.com/doi/10.1111/gcb.16811 by University Of Oklahoma, Wiley Online Library on [21/09/2023]. See the Terms and Conditions (https://onlinelibrary.wiley.com/terms-and-conditions) on Wiley Online Library for rules of use; OA articles are governed by the applicable Creative Commons License

are phylogenetically clustered (Table 1; Placella et al., 2012; Xu et al., 2018), which could reflect the fundamental differences in microbial life strategies, that is, traits driving survival, growth, and reproduction responses to environmental conditions (Barnard et al., 2013).

The phylogenetic conservation of microbial communities could be attributed to stress tolerance and competition-related traits (Goberna et al., 2014). In support of stronger stresses, the stochastic ratios of prokaryotic and fungal communities were decreased by the eP treatment (Figure 5a,b). In addition, stress tolerance genes increased in relative abundances with long-term eP (Figure 2c), reflecting higher environmental stress. For example, increases in oxygen limitation gene abundances might result from less oxygen in soil pore space or diffusing in the water film under eP (Schuur & Matson, 2001), while oxidative stress levels could be increased when microbes are under stress (Ernst et al., 2022).

The functional traits related to C degradation were shifted towards the degradation of N-rich compounds (such as chitin and protein), but not chemically C-rich compounds (such as starch, pectin, and hemicellulose, Figure 2a). These results were consistent with previous results in the JRGCE showing that 6-year eP treatment decreased hydrolase activity in degrading starch, xylan, and cellulose, but was inconsistent with a previous result of decreased chitin hydrolase activity (Henry et al., 2005). The discrepancies in chitin degradation might be due to variations in C degradation trait over different time scales or technical differences since our results reflect the genetic potentials for these processes, while enzyme activities reflect the maximum potential under ideal conditions. Degradation of N-rich molecules, including chitin and proteins, also increased along a precipitation gradient from arid to semi-arid grasslands (Feng et al., 2018), which could reflect a microbial need for acquiring N nutrients.

Viral shunt, which releases organic matter from microbial cells, plays an important role in regulating C and N cycling across different ecosystems such as marine and anaerobic digesters (Coutinho et al., 2017; Zhang et al., 2017). Consistently, the relative abundance of bacteriophage genes was increased with eP (Figure 2b and Figure S5b), and were positively correlated with genes associated with the degradation of chitin and protein and consequently affected soil total C (Figure 6a). Those results suggest that bacteriophages might play an important role in C cycling of our annual grassland ecosystem. However, we cannot yet identify the host of the bacteriophages, hindering closer examinations of interactions between bacteria and bacteriophages.

4.2 | The long-term eP treatment effects are interactively affected by elevated CO_2 and warming

Elevated CO_2 enhanced eP effects on microbial functional traits and bacterial community assemblies in this study (Figure 5a and Figure S6). One possible explanation is that CO_2 fertilization could induce higher shortages for other resources such as N and phosphorus, according to the ecological framework of (co)limitation by multiple resources (Ma et al., 2019). Also, both eCO_2 and eP could decrease root biomass (Iwasa & Roughgarden, 1984; Shaw et al., 2002), consequently reducing root input to the soil and causing soil nutrient limitation (Mason et al., 2022; Shaw et al., 2002). Consistently, we found that eP in combination with eCO_2 decreased BNPP and even NPP (Figure 1h,i). Nitrogen and phosphorus limitation was supported because we revealed enhanced degradation of N-rich compounds (Figure S6a) and decreased N cycling under eP when CO_2 was elevated (Figure S7), as well as increased phosphate limitation genes (Figure S6c). Alternatively, it is possible that eCO_2 decreases evapotranspiration, prolongs the period of water conserved in the soil, and increased soil moisture, as already observed in JRGCE and semi-arid shortgrass steppe of Colorado (Nelson et al., 2004; Zavaleta et al., 2003), hence enhancing the eP effect on microbial communities and ecosystem functioning.

Warming mitigated eP effects on soil total C and precipitation × CO_2 effects on plant root production and phosphate limitation genes (Figure 1e,l and Figure S6c). This could happen because increased evapotranspiration under warming could reduce water availability and the duration of water conserved in soil. Meanwhile, warming could enhance organic phosphorus and N mineralization to ameliorate nutrient limitation (Liu et al., 2017; Shaw & Cleveland, 2020), although the increase in N mineralization rate in response to warming has not yet been observed at our study site (Gao et al., 2021; Niboyet, Le Roux, et al., 2011).

4.3 | Microbe-plant–soil interplay is essential for mediating eP-induced soil C loss

The eP treatment reduced soil total C in the JRGCE from the 10th year of the experiment, with only a reduction in the free light fraction of soil organic matter—mainly root materials—being observed after the 6-year eP treatment (Henry et al., 2005), indicating that long-term eP exacerbated soil C loss. Since soil inorganic C content is stable in areas where mean annual precipitation is greater than 600 mm, and an increase in water availability has little effect on soil inorganic C in acidic or neutral soils (Dang et al., 2022), the decrease in soil total C in this study might be mainly attributed to the decrease in soil organic C. This result contradicts the increase in soil organic C pools with higher precipitation on the North American Great Plains (Derner & Schuman, 2007; Morrow et al., 2017). A possible explanation is that the eP effect on soil C is mediated by primary production. Increased precipitation on the Great Plains led to soil C gain by supporting plant photosynthesis (Flanagan et al., 2002), but the NPP in the JRGCE was not altered by the eP treatment due to decreases in root production, offsetting increases in shoot production (Figure 1d) (Dukes et al., 2005). Root production may decline due to reduced allocation to roots as soil resources become more available according to the optimal shoot-root C allocation theory (Iwasa & Roughgarden, 1984). Alternatively, it might be due to the suppressed root respiration as soils occasionally become waterlogged in the eP

13652486, 2023, 18, Downloaded from https://onlinelibrary.wiley.com/doi/10.1111/gcb.16811 by University Of Oklahoma, Wiley Online Library on [21/09/2023]. See the Terms and Conditions (https://onlinelibrary.wiley.com/terms-and-conditions) on Wiley Online Library for rules of use; OA articles are governed by the applicable Creative Commons License

treatment (Dukes et al., 2005). Since root exudates and decomposing root residues are large contributors to soil C pool, the decrease in root production likely explained the observed decrease in soil total C in our study (Figure 6). Notably, the decrease in root production was consistent only during the first few years (2nd–5th years) of eP treatment but not over longer terms (6th–14th years, Figure S1d). The decoupled decreases in root production and soil C (Figure S1) may indicate a legacy effect of root biomass on soil total C via C-aggregate and C-mineral associations (Sokol et al., 2022).

Microbial traits, such as resource acquisition and stress tolerance, can mediate soil C cycling (Malik et al., 2020). In resource-limited and abiotic-stressed environments, microbes tend to prioritize costly resource acquisition or stress tolerance over high growth yield, resulting in polymer decomposition and soil C loss observed in this study (Figures 5c and 6) and elsewhere (Malik et al., 2018, 2020). In addition, the enhanced microbial decomposition of soil C under eP may be responsible for soil C loss (Nielsen & Ball, 2015). Heterotrophic respiration could be positively affected by eP, especially under eCO_2 and ambient N deposition (Figure 1f). Increased water availability can stimulate microbial activity, growth, and respiration, leading to a lasting effect on soil C loss (Nielsen & Ball, 2015; Wang et al., 2015). Moreover, the eP treatment altered microbial community composition, consistent with changes in microbial community preference for different C substrates (Zhou et al., 2012). Higher abundances of fungal taxa (Figure 4 and Data S4) and C-degrading genes (Figure 2a and Figure S8) suggest that fungi become increasingly important for degrading C under the long-term eP treatment, as supported by the SEM and ABT analyses (Figure 6). Consistently, the abundances of *Eurotiales* and *Sordaiales*, the positive eP responders of fungi observed in this study (Figure 4 and Data S4), were positively correlated with the soil organic C mineralization rate, while those of *Agaricales* and *Helotiales*, the negative eP responders of fungi, were negatively correlated (Wang et al., 2021; Zhang et al., 2021). Our results coincided with the finding that potential activities of fungi-mediated C degradation enzymes, such as those degrading chitin, phosphodiester, lignin, cellulose, and xylan, were positively correlated with soil moisture (A'Bear et al., 2014). Intriguingly, the role of fungal community composition in regulating soil C was linked to the C degradation genes enriched under eP and bacteriophage genes (Figure 6a), implying possible complex interplay among bacteriophages, bacteria, and fungi in mediating the response of soil C turnover to long-term eP.

Alternatively, nutrient leaching, occurring through soil erosion or soil C migration from terrestrial to riverine ecosystems, can also contribute to soil C loss (Frank et al., 2015), though we do not suspect this to be the main cause of decreased soil C in this experiment. Although we did not measure the magnitude of C leaching directly, we could estimate it by analyzing soil N data because soil C and N leaching often happen simultaneously (He et al., 2017). The eP treatment itself did not alter N inputs either, since the supplemental water was from the domestic water supply and was added through drip irrigation and overhead sprinklers without flushing atmospheric N. Soil total N was not decreased by eP unless N deposition was elevated and the temperature was ambient (Figure 1b), suggesting that N leaching might be only evident when more N was added to soil. Therefore, change in leaching, if any, might have played a minor role in soil C loss under eP as compared to aP.

4.4 | Implications and future directions

Our findings have important implications for predicting the ecological consequences of climate change. Long-term eP altered both microbial compositions and functional traits, which differed from short-term effects (Docherty et al., 2011; Gutknecht et al., 2012). Therefore, the effects of long-term climate change on ecosystems are crucial for future studies (Melillo et al., 2017). In addition, we revealed a potential role of the viral shunt in regulating soil C cycling, underscoring the importance of including soil viruses in microbial analysis. Although numerous studies have reported that eP increases soil C storage, our results demonstrate that long-term eP combined with eCO_2 induced soil C loss in this type of water-limited annual grassland via microbe-plant–soil interplay. Therefore, a long-term increase in precipitation and CO_2 induced by climate change in some regions could generate a previously unexpected loss of soil C. This could represent an important positive feedback to climate change that has been overlooked so far. However, further research is necessary to determine whether soil C loss and associated regulating mechanisms will persist for longer time scales or in other ecosystems.

ACKNOWLEDGMENTS

The authors wish to thank the staff of the Jasper Ridge Global Change Experiment for site preservation and sampling assistance. This study was supported the National Natural Science Foundation of China grant (41825016/32161123002/42007297), Office of the Vice President for Research at the University of Oklahoma, Office of Science and Office of Biological and Environmental Research (DOE-BER) of the U.S. Department of Energy Genomic Science Program grant DE-SC0004601 and DE-SC0010715, the US National Science Foundation grant DEB-0092642/0445324, the Packard Foundation, the Morgan Family Foundation, the Second Tibetan Plateau Scientific Expedition and Research (STEP) Program grant 2019QZKK0503, Guangdong Basis and Applied Basic Research Foundation grant (2019A1515110345/2021A1515011497), Science & Technology Fundamental Resources Investigation Program grant 2019FY100700, the Key Technology R&D Program of Jiangxi Province grant 20223BBG74S02, G. Evelyn Hutchinson postdoctoral fellowship from Yale Institute for Biospheric Studies at Yale University, the Simons Foundation postdoctoral fellowship in Marine Microbial Ecology, the French Institute of Agriculture, Food and Environment Research (INRAE, ECODIV Department), and the French CNRS/INSU—EC2CO Program (project INTERACT).

CONFLICT OF INTEREST STATEMENT

The authors declare no competing interests.

13652486, 2023, 18, Downloaded from https://onlinelibrary.wiley.com/doi/10.1111/gcb.16811 by University Of Oklahoma, Wiley Online Library on [21/09/2023]. See the Terms and Conditions (https://onlinelibrary.wiley.com/terms-and-conditions) on Wiley Online Library for rules of use; OA articles are governed by the applicable Creative Commons License

DATA AVAILABILITY STATEMENT

The data that support the findings of this study are open available in Zenodo at https://doi.org/10.5281/zenodo.7964426. GeoChip data are available in the NCBI GEO database at https://www.ncbi.nlm.nih.gov/geo/, accession number GSE107168. MiSeq data are available in the NCBI SRA database at https://www.ncbi.nlm.nih.gov/sra, accession number PRJNA419455. Scripts are available at https://github.com/MengmengWang223/Microbial-functional-trait-longterm-precipitation-JRGCE.

ORCID

Mengmeng Wang https://orcid.org/0000-0002-1566-5895
Xin Sun https://orcid.org/0000-0003-0280-4283
Baichuan Cao https://orcid.org/0009-0003-8842-9193
Christopher B. Field https://orcid.org/0000-0002-1684-8247
Qun Gao https://orcid.org/0000-0002-2148-5807
Jessica L. M. Gutknecht https://orcid.org/0000-0001-7667-5272
Xue Guo https://orcid.org/0000-0002-4309-6140
Bruce A. Hungate https://orcid.org/0000-0002-7337-1887
Jiesi Lei https://orcid.org/0009-0000-0102-9540
Audrey Niboyet https://orcid.org/0000-0003-3355-706X
Xavier Le Roux https://orcid.org/0000-0001-9695-0825
Zhou Shi https://orcid.org/0000-0002-9149-1540
Wensheng Shu https://orcid.org/0000-0002-8743-1705
Mengting Yuan https://orcid.org/0000-0003-0017-3908
Jizhong Zhou https://orcid.org/0000-0003-2014-0564
Yunfeng Yang https://orcid.org/0000-0001-8274-6196

REFERENCES

Abarenkov, K., Zirk, A., Piirmann, T., Pöhönen, R., Ivanov, F., Nilsson, R. H., & Kõljalg, U. (2021). *UNITE QIIME release for fungi*. UNITE Community.

A'bear, A. D., Jones, T. H., Kandeler, E., & Boddy, L. (2014). Interactive effects of temperature and soil moisture on fungal-mediated wood decomposition and extracellular enzyme activity. *Soil Biology and Biochemistry*, *70*, 151–158.

Barnard, R., Le Roux, X., Hungate, B. A., Cleland, E. E., Blankinship, J. C., Barthes, L., & Leadley, P. W. (2006). Several components of global change alter nitrifying and denitrifying activities in an annual grassland. *Functional Ecology*, *20*, 557–564.

Barnard, R., Osborne, C. A., & Firestone, M. K. (2013). Responses of soil bacterial and fungal communities to extreme desiccation and rewetting. *The ISME Journal*, *7*, 2229–2241.

Bolyen, E., Rideout, J. R., Dillon, M. R., Bokulich, N. A., Abnet, C. C., Al-Ghalith, G. A., Alexander, H., Alm, E. J., Arumugam, M., Asnicar, F., Bai, Y., Bisanz, J. E., Bittinger, K., Brejnrod, A., Brislawn, C. J., Brown, C. T., Callahan, B. J., Caraballo-Rodríguez, A. M., Chase, J., … Caporaso, J. G. (2019). Reproducible, interactive, scalable and extensible microbiome data science using QIIME 2. *Nature Biotechnology*, *37*, 852–857.

Brown, J. R., Blankinship, J. C., Niboyet, A., van Groenigen, K. J., Dijkstra, P., Le Roux, X., Leadley, P. W., & Hungate, B. A. (2012). Effects of multiple global change treatments on soil N_2O fluxes. *Biogeochemistry*, *109*, 85–100.

Chou, W. W., Silver, W. L., Jackson, R. D., Thompson, A. W., & Allen-Diaz, B. (2008). The sensitivity of annual grassland carbon cycling to the quantity and timing of rainfall. *Global Change Biology*, *14*, 1382–1394.

Corringham, T. W., Ralph, F. M., Gershunov, A., Cayan, D. R., & Talbot, C. A. (2019). Atmospheric rivers drive flood damages in the western United States. *Science Advances*, *5*, eaax4631.

Coutinho, F. H., Silveira, C. B., Gregoracci, G. B., Thompson, C. C., Edwards, R. A., Brussaard, C. P. D., Dutilh, B. E., & Thompson, F. L. (2017). Marine viruses discovered via metagenomics shed light on viral strategies throughout the oceans. *Nature Communications*, *8*, 15955.

Dahlin, K. M., Asner, G. P., & Field, C. B. (2013). Environmental and community controls on plant canopy chemistry in a Mediterranean-type ecosystem. *Proceedings of the National Academy of Sciences of the United States of America*, *110*, 6895–6900.

Dang, C., Kong, F., Li, Y., Jiang, Z., & Xi, M. (2022). Soil inorganic carbon dynamic change mediated by anthropogenic activities: An integrated study using meta-analysis and random forest model. *Science of the Total Environment*, *835*, 155463.

De'ath, G. (2007). Boosted trees for ecological modeling and prediction. *Ecology*, *88*, 243–251.

Derner, J. D., & Schuman, G. E. (2007). Carbon sequestration and rangelands: A synthesis of land management and precipitation effects. *Journal of Soil and Water Conservation*, *62*, 77–85.

Docherty, K. M., Balser, T. C., Bohannan, B. J. M., & Gutknecht, J. L. M. (2011). Soil microbial responses to fire and interacting global change factors in a California annual grassland. *Biogeochemistry*, *109*, 63–83.

Dukes, J. S., Chiariello, N. R., Cleland, E. E., Moore, L. A., Shaw, M. R., Thayer, S., Tobeck, T., Mooney, H. A., & Field, C. B. (2005). Responses of grassland production to single and multiple global environmental changes. *PLoS Biology*, *3*, e319.

Edgar, R. C. (2018). Updating the 97% identity threshold for 16S ribosomal RNA OTUs. *Bioinformatics*, *34*, 2371–2375.

Ernst, L., Steinfeld, B., Barayeu, U., Klintzsch, T., Kurth, M., Grimm, D., Dick, T. P., Rebelein, J. G., Bischofs, I. B., & Keppler, F. (2022). Methane formation driven by reactive oxygen species across all living organisms. *Nature*, *603*, 482–487.

Falloon, P., Jones, C. D., Ades, M., & Paul, K. (2011). Direct soil moisture controls of future global soil carbon changes: An important source of uncertainty. *Global Biogeochemical Cycles*, *25*, GB3010.

Feng, J., Turner, B. L., Wei, K., Tian, J., Chen, Z., Lü, X., Wang, C., & Chen, L. (2018). Divergent composition and turnover of soil organic nitrogen along a climate gradient in arid and semiarid grasslands. *Geoderma*, *327*, 36–44.

Flanagan, L. B., Wever, L. A., & Carlson, P. J. (2002). Seasonal and interannual variation in carbon dioxide exchange and carbon balance in a northern temperate grassland. *Global Change Biology*, *8*, 599–615.

Fouquier, J., Rideout, J. R., Bolyen, E., Chase, J., Shiffer, A., McDonald, D., Knight, R., Caporaso, J. G., & Kelley, S. T. (2016). Ghost-tree: Creating hybrid-gene phylogenetic trees for diversity analyses. *Microbiome*, *4*, 11.

Frank, D., Reichstein, M., Bahn, M., Thonicke, K., Frank, D., Mahecha, M. D., Smith, P., Velde, M., Vicca, S., Babst, F., Beer, C., Buchmann, N., Canadell, J. G., Ciais, P., Cramer, W., Ibrom, A., Miglietta, F., Poulter, B., Rammig, A., … Zscheischler, J. (2015). Effects of climate extremes on the terrestrial carbon cycle: Concepts, processes and potential future impacts. *Global Change Biology*, *21*, 2861–2880.

Gao, Y., Ding, J., Yuan, M., Chiariello, N., Docherty, K., Field, C., Gao, Q., Gu, B., Gutknecht, J., Hungate, B. A., Le Roux, X., Niboyet, A., Qi, Q., Shi, Z., Zhou, J., & Yang, Y. (2021). Long-term warming in a Mediterranean-type grassland affects soil bacterial functional potential but not bacterial taxonomic composition. *npj Biofilms and Microbiomes*, *7*, 17.

Goberna, M., Navarro-Cano, J. A., Valiente-Banuet, A., Garcia, C., & Verdu, M. (2014). Abiotic stress tolerance and competition-related

13652486, 2023, 18, Downloaded from https://onlinelibrary.wiley.com/doi/10.1111/gcb.16811 by University Of Oklahoma, Wiley Online Library on [21/09/2023]. See the Terms and Conditions (https://onlinelibrary.wiley.com/terms-and-conditions) on Wiley Online Library for rules of use; OA articles are governed by the applicable Creative Commons License

traits underlie phylogenetic clustering in soil bacterial communities. *Ecology Letters*, *17*, 1191–1201.

Gulev, S. K., Thorne, P. W., Ahn, J., Dentener, F. J., Domingues, C. M., Gerland, S., Gong, D., Kaufman, D. S., Nnamchi, H. C., Quaas, J., Rivera, J. A., Sathyendranath, S., Smith, S. L., Trewin, B., von Schuckmann, K., & Vos, R. S. (2021). Changing state of the climate system. In V. Masson–Delmotte, P. Zhai, A. Pirani, S. L. Connors, C. Péan, S. Berger, N. Caud, Y. Chen, L. Goldfarb, M. I. Gomis, M. Huang, K. Leitzell, E. Lonnoy, J. B. R. Matthews, T. K. Maycock, T. Waterfield, O. Yelekçi, R. Yu, & B. Zhou (Eds.), *Climate change 2021: The physical science basis. Contribution of working group I to the sixth assessment report of the intergovernmental panel on climate change*. Cambridge University Press.

Guo, X., Feng, J., Shi, Z., Zhou, X., Yuan, M., Tao, X., Hale, L., Yuan, T., Wang, J., Qin, Y., Zhou, A., Fu, Y., Wu, L., He, Z., van Nostrand, J. D., Ning, D., Liu, X., Luo, Y., Tiedje, J. M., … Zhou, J. (2018). Climate warming leads to divergent succession of grassland microbial communities. *Nature Climate Change*, *8*, 813–818.

Guo, X., Zhou, X., Hale, L., Yuan, M., Ning, D., Feng, J., Shi, Z., Li, Z., Feng, B., Gao, Q., Wu, L., Shi, W., Zhou, A., Fu, Y., Wu, L., He, Z., van Nostrand, J. D., Qiu, G., Liu, X., … Zhou, J. (2019). Climate warming accelerates temporal scaling of grassland soil microbial biodiversity. *Nature Ecology & Evolution*, *3*, 612–619.

Gutknecht, J. L. M., Field, C. B., & Balser, T. C. (2012). Microbial communities and their responses to simulated global change fluctuate greatly over multiple years. *Global Change Biology*, *18*, 2256–2269.

He, Y., Lehndorff, E., Amelung, W., Wassmann, R., Alberto, M. C., Von Unold, G., & Siemens, J. (2017). Drainage and leaching losses of nitrogen and dissolved organic carbon after introducing maize into a continuous paddy-rice crop rotation. *Agriculture, Ecosystems & Environment*, *249*, 91–100.

Henry, H. A., Juarez, J. D., Field, C. B., & Vitousek, P. M. (2005). Interactive effects of elevated CO_2, N deposition and climate change on extracellular enzyme activity and soil density fractionation in a California annual grassland. *Global Change Biology*, *11*, 1808–1815.

Horz, H.-P., Barbrook, A., Field, C. B., & Bohannan, B. J. (2004). Ammonia-oxidizing bacteria respond to multifactorial global change. *Proceedings of the National Academy of Sciences of the United States of America*, *101*, 15136–15141.

Hubbell, S. P. (2001). *The unified neutral theory of biodiversity and biogeography (MPB-32)*. Princeton University Press.

Huntington, T. G. (2006). Evidence for intensification of the global water cycle: Review and synthesis. *Journal of Hydrology*, *319*, 83–95.

Iwasa, Y., & Roughgarden, J. (1984). Shoot/root balance of plants: Optimal growth of a system with many vegetative organs. *Theoretical Population Biology*, *25*, 78–105.

Le Roux, X., Bouskill, N. J., Niboyet, A., Niboyet, A., Barthes, L., Dijkstra, P., Field, C. B., Hungate, B. A., Lerondelle, C., Pommier, T., Tang, J., Terada, A., Tourna, M., & Poly, F. (2016). Predicting the responses of soil nitrite-oxidizers to multi-factorial global change: A trait-based approach. *Frontiers in Microbiology*, *7*, 628.

Liu, Y., Wang, C., He, N., Wen, X., Gao, Y., Li, S., Niu, S., Butterbach-Bahl, K., Luo, Y., & Yu, G. (2017). A global synthesis of the rate and temperature sensitivity of soil nitrogen mineralization: Latitudinal patterns and mechanisms. *Global Change Biology*, *23*, 455–464.

Louca, S., & Doebeli, M. (2018). Efficient comparative phylogenetics on large trees. *Bioinformatics*, *34*, 1053–1055.

Love, M. I., Huber, W., & Anders, S. (2014). Moderated estimation of fold change and dispersion for RNA-seq data with DESeq2. *Genome Biology*, *15*, 550.

Ma, B., Zhou, X., Zhang, Q., Qin, M., Hu, L., Yang, K., Xie, Z., Ma, W., Chen, B., Feng, H., Liu, Y., Du, G., Ma, X., & Le Roux, X. (2019). How do soil micro-organisms respond to N, P and NP additions? Application of the ecological framework of (co-)limitation by multiple resources. *Journal of Ecology*, *107*, 2329–2345.

Magoč, T., & Salzberg, S. L. (2011). FLASH: Fast length adjustment of short reads to improve genome assemblies. *Bioinformatics*, *27*, 2957–2963.

Malik, A. A., Martiny, J. B. H., Brodie, E. L., Martiny, A. C., Treseder, K. K., & Allison, S. D. (2020). Defining trait-based microbial strategies with consequences for soil carbon cycling under climate change. *The ISME Journal*, *14*, 1–9.

Malik, A. A., Puissant, J., Buckeridge, K. M., Goodall, T., Jehmlich, N., Chowdhury, S., Gweon, H. S., Peyton, J. M., Mason, K. E., van Agtmaal, M., Blaud, A., Clark, I. M., Whitaker, J., Pywell, R. F., Ostle, N., Gleixner, G., & Griffiths, R. I. (2018). Land use driven change in soil pH affects microbial carbon cycling processes. *Nature Communications*, *9*, 1–10.

Marti, J. A., Gorley, R. N., & Clarke, R. K. (2008). *PERMANOVA+ for PRIMER: Guide to software and statistical methods*. Primer-e.

Martiny, A. C., Treseder, K., & Pusch, G. (2013). Phylogenetic conservatism of functional traits in microorganisms. *The ISME Journal*, *7*, 830–838.

Mason, R. E., Craine, J. M., Lany, N. K., Jonard, M., Ollinger, S. V., Groffman, P. M., Fulweiler, R. W., Angerer, J., Read, Q. D., Reich, P. B., Templer, P. H., & Elmore, A. J. (2022). Evidence, causes, and consequences of declining nitrogen availability in terrestrial ecosystems. *Science*, *376*, eabh3767.

Melillo, J. M., Frey, S. D., DeAngelis, K., Werner, W. J., Bernard, M. J., Bowles, F. P., Pold, G., Knorr, M. A., & Grandy, A. S. (2017). Long-term pattern and magnitude of soil carbon feedback to the climate system in a warming world. *Science*, *358*, 101–105.

Morrow, J. G., Huggins, D. R., & Reganold, J. P. (2017). Climate change predicted to negatively influence surface soil organic matter of dryland cropping systems in the inland Pacific northwest, USA. *Frontiers in Ecology and Evolution*, *5*, 10.

Nelson, J. A., Morgan, J. A., Lecain, D. R., Mosier, A. R., Milchunas, D. G., & Parton, B. A. (2004). Elevated CO_2 increases soil moisture and enhances plant water relations in a long-term field study in semi-arid shortgrass steppe of Colorado. *Plant and Soil*, *259*, 169–179.

Niboyet, A., Brown, J. R., Dijkstra, P., Blankinship, J. C., Leadley, P. W., Le Roux, X., Barthes, L., Barnard, R. L., Field, C. B., & Hungate, B. A. (2011). Global change could amplify fire effects on soil greenhouse gas emissions. *PLoS One*, *6*, e20105.

Niboyet, A., Le Roux, X., Dijkstra, P., Hungate, B. A., Barthes, L., Blankinship, J. C., Brown, J. R., Field, C. B., & Leadley, P. W. (2011). Testing interactive effects of global environmental changes on soil nitrogen cycling. *Ecosphere*, *2*, art56.

Nielsen, U. N., & Ball, B. A. (2015). Impacts of altered precipitation regimes on soil communities and biogeochemistry in arid and semi-arid ecosystems. *Global Change Biology*, *21*, 1407–1421.

Ning, D., Deng, Y., Tiedje, J. M., & Zhou, J. (2019). A general framework for quantitatively assessing ecological stochasticity. *Proceedings of the National Academy of Sciences of the United States of America*, *116*, 16892–16898.

Ochoa-Hueso, R., Arca, V., Delgado-Baquerizo, M., Hamonts, K., Piñeiro, J., Serrano-Grijalva, L., Shawyer, J., & Power, S. A. (2020). Links between soil microbial communities, functioning, and plant nutrition under altered rainfall in Australian grassland. *Ecological Monographs*, *90*, e01424.

Placella, S. A., Brodie, E. L., & Firestone, M. K. (2012). Rainfall-induced carbon dioxide pulses result from sequential resuscitation of phylogenetically clustered microbial groups. *Proceedings of the National Academy of Sciences of the United States of America*, *109*, 10931–10936.

Price, M. N., Dehal, P. S., & Arkin, A. P. (2010). FastTree 2—Approximately maximum-likelihood trees for large alignments. *PLoS One*, *5*, e9490.

Prosser, J. I., Bohannan, B. J., Curtis, T. P., Ellis, R. J., Firestone, M. K., Freckleton, R. P., Green, J. L., Green, L. E., Killham, K., Lennon, J. J., Osborn, A. M., Solan, M., van der Gast, C., & Young, J. P. (2007). The role of ecological theory in microbial ecology. *Nature Reviews Microbiology*, *5*, 384–392.

13652486, 2023, 18, Downloaded from https://onlinelibrary.wiley.com/doi/10.1111/gcb.16811 by University Of Oklahoma, Wiley Online Library on [21/09/2023]. See the Terms and Conditions (https://onlinelibrary.wiley.com/terms-and-conditions) on Wiley Online Library for rules of use; OA articles are governed by the applicable Creative Commons License

Qi, Q., Haowei, Y., Zhang, Z., van Nostrand, J. D., Wu, L., Guo, X., Feng, J., Wang, M., Yang, S., Zhao, J., Gao, Q., Zhang, Q., Zhao, M., Xie, C., Ma, Z., He, J. S., Chu, H., Huang, Y., Zhou, J., & Yang, Y. (2021). Microbial functional responses explain alpine soil carbon fluxes under future climate scenarios. *mBio*, *12*, e00761–e00720.

Quast, C., Pruesse, E., Yilmaz, P., Gerken, J., Schweer, T., Yarza, P., Peplies, J., & Glöckner, F. O. (2013). The SILVA ribosomal RNA gene database project: Improved data processing and web-based tools. *Nucleic Acids Research*, *41*, D590–D596.

Reichstein, M., Bahn, M., Ciais, P., Frank, D., Mahecha, M. D., Seneviratne, S. I., Zscheischler, J., Beer, C., Buchmann, N., Frank, D. C., Papale, D., Rammig, A., Smith, P., Thonicke, K., van der Velde, M., Vicca, S., Walz, A., & Wattenbach, M. (2013). Climate extremes and the carbon cycle. *Nature*, *500*, 287–295.

Rosseel, Y. (2012). Lavaan: An R package for structural equation modeling. *Journal of Statistical Software*, *48*, 1–36.

Schuur, E. A., & Matson, P. A. (2001). Net primary productivity and nutrient cycling across a mesic to wet precipitation gradient in Hawaiian montane forest. *Oecologia*, *128*, 431–442.

Shaw, A. N., & Cleveland, C. C. (2020). The effects of temperature on soil phosphorus availability and phosphatase enzyme activities: A cross-ecosystem study from the tropics to the Arctic. *Biogeochemistry*, *151*, 113–125.

Shaw, M. R., Zavaleta, E. S., Chiariello, N. R., Cleland, E. E., Mooney, H. A., & Field, C. B. (2002). Grassland responses to global environmental changes suppressed by elevated CO_2. *Science*, *298*, 1987–1990.

Shi, Y., Wang, J., Ao, Y., Han, J., Guo, Z., Liu, X., Zhang, J., Mu, C., & Le Roux, X. (2021). Responses of soil N_2O emissions and their abiotic and biotic drivers to altered rainfall regimes and co-occurring wet N deposition in a semi-arid grassland. *Global Change Biology*, *27*, 4894–4908.

Sokol, N. W., Slessarev, E., Marschmann, G. L., Nicolas, A., Blazewicz, S. J., Brodie, E. L., Firestone, M. K., Foley, M. M., Hestrin, R., Hungate, B. A., Koch, B. J., Stone, B. W., Sullivan, M. B., Zablocki, O., LLNL Soil Microbiome Consortium, Trubl, G., McFarlane, K., Stuart, R., Nuccio, E., … Pett-Ridge, J. (2022). Life and death in the soil microbiome: How ecological processes influence biogeochemistry. *Nature Reviews Microbiology*, *20*, 415–430.

Stevenson, S., Coats, S., Touma, D., Cole, J., Lehner, F., Fasullo, J., & Otto-Bliesner, B. (2022). Twenty-first century hydroclimate: A continually changing baseline, with more frequent extremes. *Proceedings of the National Academy of Sciences of the United States of America*, *119*, e2108124119.

Strong, A. L., Johnson, T. P., Chiariello, N. R., & Field, C. B. (2017). Experimental fire increases soil carbon dioxide efflux in a grassland long-term multifactor global change experiment. *Global Change Biology*, *23*, 1975–1987.

Sullivan, M. J., Thomsen, M. A., & Suttle, K. B. (2016). Grassland responses to increased rainfall depend on the timescale of forcing. *Global Change Biology*, *22*, 1655–1665.

Tiedje, J. M., Bruns, M. A., Casadevall, A., Criddle, C. S., Eloe-Fadrosh, E., Karl, D. M., Nguyen, N. K., & Zhou, J. (2022). Microbes and climate change: A research prospectus for the future. *mBio*, *13*, e00800–e00822.

Wang, M., Ding, J., Sun, B., Zhang, J., Wyckoff, K. N., Yue, H., Zhao, M., Liang, Y., Wang, X., Wen, C., Zhou, J., & Yang, Y. (2018). Microbial responses to inorganic nutrient amendment overridden by warming: Consequences on soil carbon stability. *Environmental Microbiology*, *20*, 2509–2522.

Wang, R., Dorodnikov, M., Yang, S., Zhang, Y., Filley, T. R., Turco, R. F., Zhang, Y., Xu, Z., Li, H., & Jiang, Y. (2015). Responses of enzymatic activities within soil aggregates to 9-year nitrogen and water addition in a semi-arid grassland. *Soil Biology and Biochemistry*, *81*, 159–167.

Wang, X., Bian, Q., Jiang, Y., Zhu, L., Chen, Y., Liang, Y., & Sun, B. (2021). Organic amendments drive shifts in microbial community structure and keystone taxa which increase C mineralization across aggregate size classes. *Soil Biology and Biochemistry*, *153*, 108062.

Williamson, K. E., Fuhrmann, J. J., Wommack, K. E., & Radosevich, M. (2017). Viruses in soil ecosystems: An unknown quantity within an unexplored territory. *Annual Review of Virology*, *4*, 201–219.

Xu, L., Naylor, D., Dong, Z., Simmons, T., Pierroz, G., Hixson, K. K., Kim, Y. M., Zink, E. M., Engbrecht, K. M., Wang, Y., Gao, C., DeGraaf, S., Madera, M. A., Sievert, J. A., Hollingsworth, J., Birdseye, D., Scheller, H. V., Hutmacher, R., Dahlberg, J., … Coleman-Derr, D. (2018). Drought delays development of the sorghum root microbiome and enriches for monoderm bacteria. *Proceedings of the National Academy of Sciences of the United States of America*, *115*, E4284–E4293.

Yang, S., Zheng, Q., Yang, Y., Yuan, M., Ma, X., Chiariello, N. R., Docherty, K. M., Field, C. B., Gutknecht, J. L. M., Hungate, B. A., Niboyet, A., Le Roux, X., & Zhou, J. (2020). Fire affects the taxonomic and functional composition of soil microbial communities, with cascading effects on grassland ecosystem functioning. *Global Change Biology*, *26*, 431–442.

Yang, Y., Gao, Y., Wang, S., Xu, D., Yu, H., Wu, L., Lin, Q., Hu, Y., Li, X., He, Z., Deng, Y., & Zhou, J. (2014). The microbial gene diversity along an elevation gradient of the Tibetan grassland. *The ISME Journal*, *8*, 430–440.

Zavaleta, E. S., Shaw, M. R., Chiariello, N. R., Mooney, H. A., & Field, C. B. (2003). Additive effects of simulated climate changes, elevated CO_2, and nitrogen deposition on grassland diversity. *Proceedings of the National Academy of Sciences of the United States of America*, *100*, 7650–7654.

Zhang, J., Gao, Q., Zhang, Q., Wang, T., Yue, H., Wu, L., Shi, J., Qin, Z., Zhou, J., Zuo, J., & Yang, Y. (2017). Bacteriophage-prokaryote dynamics and interaction within anaerobic digestion processes across time and space. *Microbiome*, *5*, 57.

Zhang, S., Fang, Y., Luo, Y., Li, Y., Ge, T., Wang, Y., Wang, H., Yu, B., Song, X., Chen, J., Zhou, J., Li, Y., & Chang, S. X. (2021). Linking soil carbon availability, microbial community composition and enzyme activities to organic carbon mineralization of a bamboo forest soil amended with pyrogenic and fresh organic matter. *Science of the Total Environment*, *801*, 149717.

Zhou, J., Bruns, M. A., & Tiedje, J. M. (1996). DNA recovery from soils of diverse composition. *Applied and Environmental Microbiology*, *62*, 316–322.

Zhou, J., Xue, K., Xie, J., Deng, Y., Wu, L., Cheng, X., Fei, S., Deng, S., He, Z., van Nostrand, J. D., & Luo, Y. (2012). Microbial mediation of carbon-cycle feedbacks to climate warming. *Nature Climate Change*, *2*, 106–110.

Zhu, K., Chiariello, N. R., Tobeck, T., Fukami, T., & Field, C. B. (2016). Nonlinear, interacting responses to climate limit grassland production under global change. *Proceedings of the National Academy of Sciences of the United States of America*, *113*, 10589–10594.

SUPPORTING INFORMATION

Additional supporting information can be found online in the Supporting Information section at the end of this article.

How to cite this article: Wang, M., Sun, X., Cao, B., Chiariello, N. R., Docherty, K. M., Field, C. B., Gao, Q., Gutknecht, J. L. M., Guo, X., He, G., Hungate, B. A., Lei, J., Niboyet, A., Le Roux, X., Shi, Z., Shu, W., Yuan, M., Zhou, J., & Yang, Y. (2023). Long-term elevated precipitation induces grassland soil carbon loss via microbe-plant–soil interplay. *Global Change Biology*, *29*, 5429–5444. https://doi.org/10.1111/gcb.16811

13652486, 2023, 18, Downloaded from https://onlinelibrary.wiley.com/doi/10.1111/gcb.16811 by University Of Oklahoma, Wiley Online Library on [21/09/2023]. See the Terms and Conditions (https://onlinelibrary.wiley.com/terms-and-conditions) on Wiley Online Library for rules of use; OA articles are governed by the applicable Creative Commons License